

Short communication

Facile synthesis of imidazoles by an efficient and eco-friendly heterogeneous catalytic system constructed of Fe₃O₄ and Cu₂O nanoparticles, and guarana as a natural basis

Zahra Varzi, Mir Saeed Esmaeili¹, Reza Taheri-Ledari, Ali Maleki*

Catalysts and Organic Synthesis Research Laboratory, Department of Chemistry, Iran University of Science and Technology, Tehran 16846-13114, Iran



ARTICLE INFO

Keywords:

Copper nanoparticles
Guarana
Organometallic nanocomposite
Heterogeneous nanocatalyst
Biopolymer texture
Imidazole reaction

ABSTRACT

In this study, an efficient hybrid nanocatalyst made of guar gum (guarana, as a natural basis), magnetic iron oxide nanoparticles, and copper(I) oxide nanoparticles (Cu₂O NPs) is fabricated and suitably applied for catalyzing the multicomponent (three- and four-component) synthesis reactions of imidazole derivatives. Here, an easy preparation strategy for this novel catalytic system (Cu₂O/Fe₃O₄@guarana) is presented. Then, the application of this catalytic system for the synthesis of imidazole derivatives is precisely investigated. For this purpose, ultrasonication is introduced as an efficient and fast method. In summary, the high catalytic efficiency of Cu₂O/Fe₃O₄@guarana nanocomposite is well demonstrated by high reaction yields obtained in the presence of a small amount of this nanocomposite, under mild conditions. Wide active surface area, substantial magnetic behavior, excellent heterogeneity, suitable stability, well reusability, and etc. have distinguished this catalytic system as an instrumental tool for facilitating the complex synthetic reactions.

1. Introduction

In two recent decades, attentions to heterogeneous nanoscale systems have been amazingly increased due to their substantial effectiveness on various types of the scientific studies. For instance, in medicine, they are extremely used for targeted drug delivery, in which the desired medication is delivered to the target tissue with high selectivity [1–3]. In the field of the natural energies, they have been widely applied for fabrication of the novel devices (like solar cells) with higher efficiencies. For this purpose, the internal layers of a device is manipulated via re-composition of the heterogeneous nanoscale materials [4]. In fact, nano scaling affects the band gap of the ingredients that are involved in an electronic device [5,6]. Moreover, the nanoscale heterogeneous materials have been used for catalytic aims. So far, numerous nanocatalysts with high performances as great alternatives for traditional homogeneous catalytic systems have been designed and introduced to the science world [7–14]. In other words, the ancient generation of the catalytic systems (organocatalyst) is being replaced by next generation (heterogeneous nanocatalyst), which includes several excellences. The first and foremost advantage is heterogeneity that leads to convenient separation and purification processes. In fact, complex conventional

separation processes like antisolvent, column chromatography, recrystallization and etc. are practically removed from the procedures [15,16]. Providing wide surface active areas (through nano scaling), shortening the reaction times (through high performances), and high biocompatibility and biodegradability (through involving the natural resources for designing a catalytic system), could also be referred as additional advantages for this newly emerged generation of the catalytic systems [17,18]. Recently, magnetic property has also been added to the heterogeneous catalytic systems through the composition of the magnetic ingredients like iron oxide nanoparticles (Fe₃O₄ NPs), which creates more convenience in the separation processes. In this regard, several magnetic catalytic systems have been designed and suitably applied for various catalytic applications [19–22]. Furthermore, the catalytic activity of these heterogeneous particles could be enhanced through simultaneously applying other energy resources like ultrasound waves [23,24]. Thus, in this study, we try to design an efficient heterogeneous system, in which Fe₃O₄ NPs are well composed with other components to make a magnetic catalytic system.

For immobilization of the NPs in the composited form, polymeric and fibrous matrices are usually used [25]. In this case, polymeric textures with natural resources are typically preferred due to their

* Corresponding author.

E-mail address: maleki@iust.ac.ir (A. Maleki).¹ Co-first author.

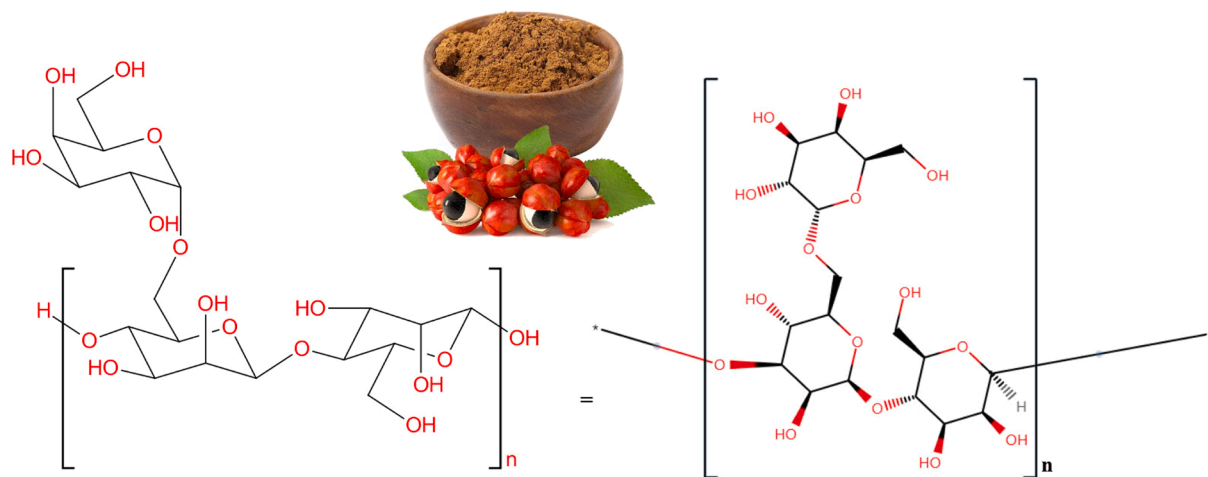


Fig. 1. The chemical structure of the guarana natural polymeric strand.

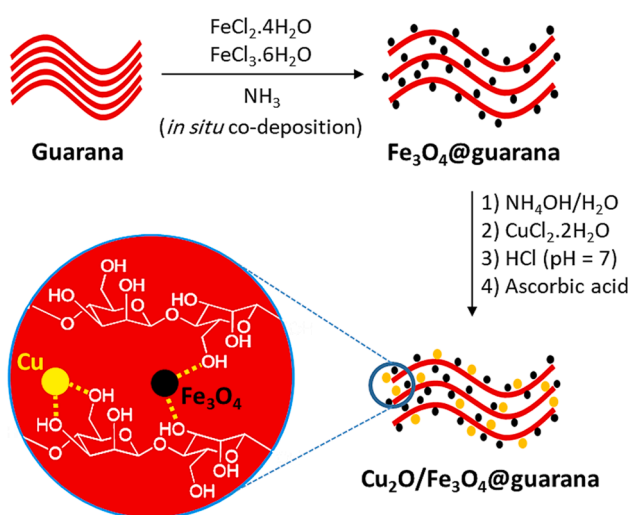


Fig. 2. Preparation route of $\text{Cu}_2\text{O}/\text{Fe}_3\text{O}_4$ @guarana nanocomposite.

biocompatibility and biodegradability, and also nontoxicity that well meet the principles of the green chemistry [26]. As well, the polymer's textures could be chemically functionalized through the existence of the functional groups (like hydroxyl) [27]. In this regard, we chose "Guarana" (also called guar gum) that is considered as an appropriate additive in many processed foods [28]. From chemical aspect, there are several hydroxyl groups in the guarana's structure that provide a suitable substrate for the composition of the other essential components (Fig. 1). From biological aspect, guarana is extracted from a plant resource and not only produces no toxic substances, but also adds high biocompatibility to our catalytic system.

However, in this work, we have made an effort to suitably employ guarana (as a natural substrate) for immobilization of the Fe_3O_4 NPs and copper(I) oxide (Cu_2O) NPs. For this purpose, a convenient *in situ* process has been applied, through which guarana textures are well magnetized with the composed Fe_3O_4 NPs. Then, Cu_2O NPs are formed and well immobilized between the textures of guarana. In fact, Cu_2O NPs are the main active catalytic sites of our designed system ($\text{Cu}_2\text{O}/\text{Fe}_3\text{O}_4$ @guarana), which provide constructive electronic interactions between the involved components in three- and four-component synthesis reactions of imidazole derivatives. Herein, precise optimization

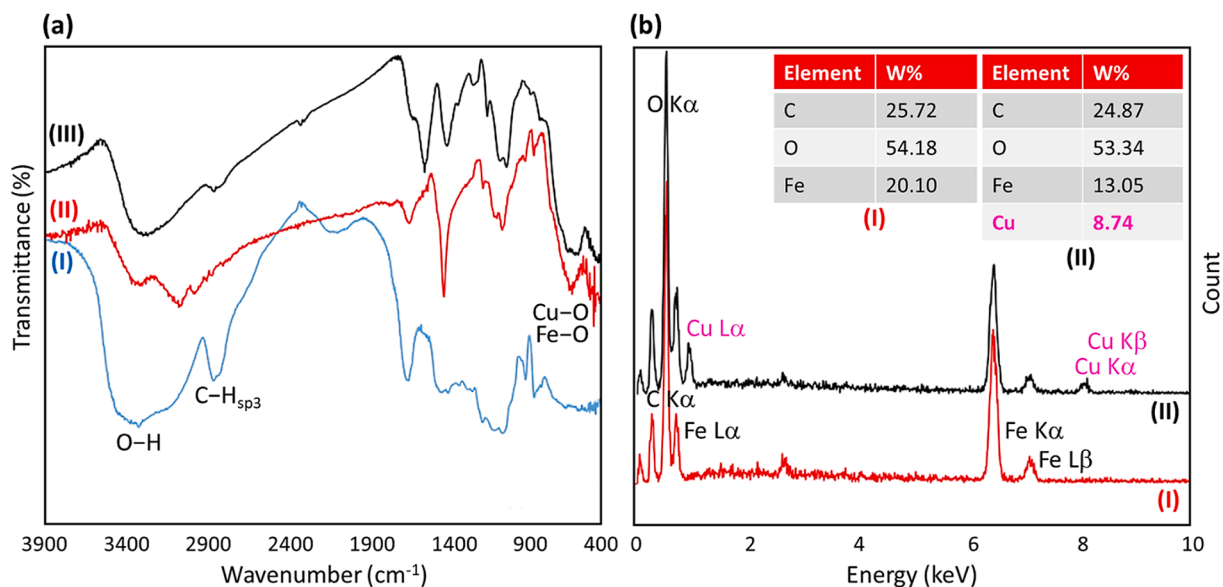


Fig. 3. (a) FT-IR spectra of the neat guarana (I), Fe_3O_4 @guarana nanocomposite (II), and $\text{Cu}_2\text{O}/\text{Fe}_3\text{O}_4$ @guarana nanocomposite (III), and (b) EDX spectra and the elemental quantitative ratios tables of Fe_3O_4 @guarana nanocomposite (I), and $\text{Cu}_2\text{O}/\text{Fe}_3\text{O}_4$ @guarana nanocomposite (II).

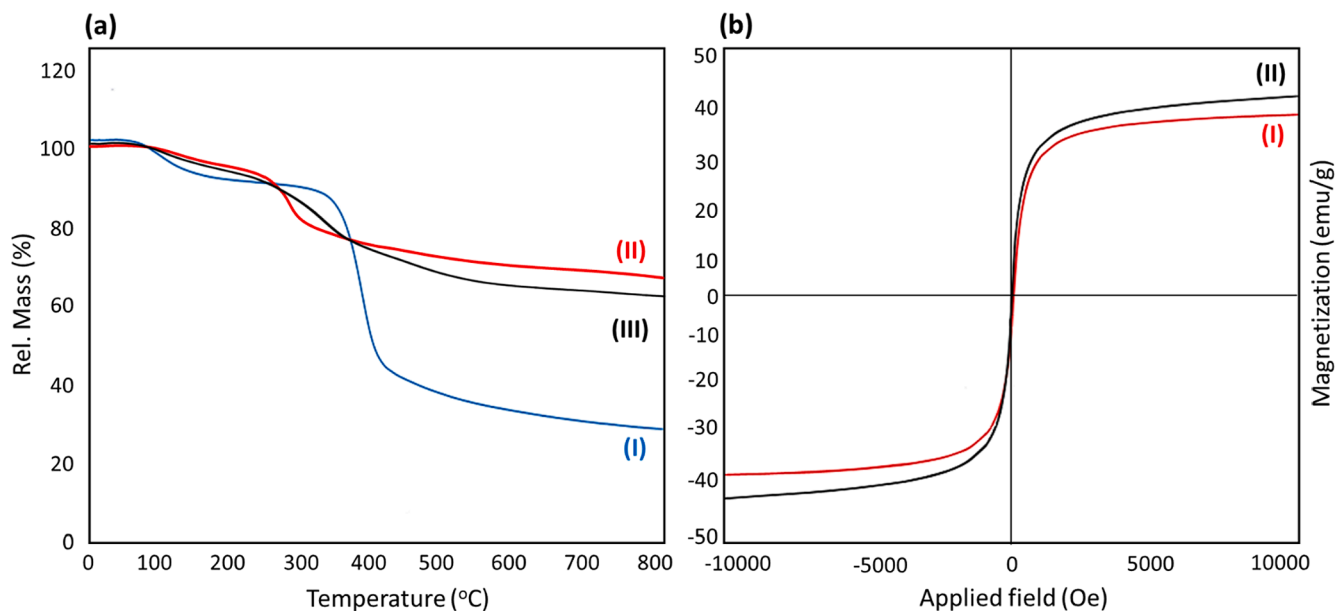


Fig. 4. (a) TGA curves of the neat guarana (I), Fe_3O_4 @guarana nanocomposite (II), and $\text{Cu}_2\text{O}/\text{Fe}_3\text{O}_4$ @guarana nanocomposite (III), and VSM M–H curves of Fe_3O_4 @guarana nanocomposite (I), and $\text{Cu}_2\text{O}/\text{Fe}_3\text{O}_4$ @guarana nanocomposite (II) (recorded at room temperature).

and comparisons have been made to highlight the performance of the fabricated $\text{Cu}_2\text{O}/\text{Fe}_3\text{O}_4$ @guarana. In this study, ultrasonication is introduced as the best applicable conditions for the synthesis of imidazoles in the presence of $\text{Cu}_2\text{O}/\text{Fe}_3\text{O}_4$ @guarana heterogeneous catalytic system.

2. Results and discussion

2.1. Preparation of the $\text{Cu}_2\text{O}/\text{Fe}_3\text{O}_4$ @guarana nanocomposite

The schematic of the preparation route of $\text{Cu}_2\text{O}/\text{Fe}_3\text{O}_4$ @guarana nanocomposite is presented in Fig. 2. As a fast and concise review, it is observed that guarana textures are well magnetized with Fe_3O_4 NPs via

an *in situ* co-deposition process. For this purpose, the chloride salts of iron(II) and iron(III) have been used in basic conditions ($\text{pH} \sim 12$), provided by ammonia solution [29,30]. Then, the reaction medium is neutralized by HCl (0.1 M) and the chloride salt of copper(II) in the presence of ascorbic acid [31]. After completion of the preparation reaction, the fabricated final product has been conveniently separated (by using an external magnet at the bottom of the flask), and well washed to remove the excess ions.

2.2. Characterization of the $\text{Cu}_2\text{O}/\text{Fe}_3\text{O}_4$ @guarana nanocomposite

As the first identification method, Fourier-transform infrared (FT-IR) spectroscopy was used (Fig. 3a). As can be seen in the spectra, the peak

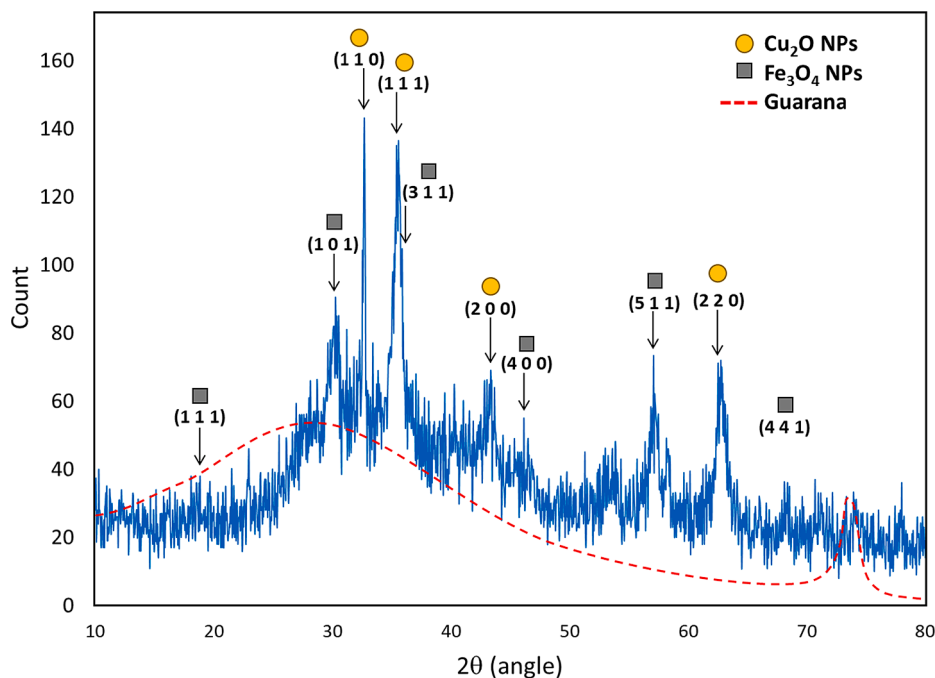


Fig. 5. XRD pattern of the fabricated $\text{Cu}_2\text{O}/\text{Fe}_3\text{O}_4$ @guarana nanocomposite.

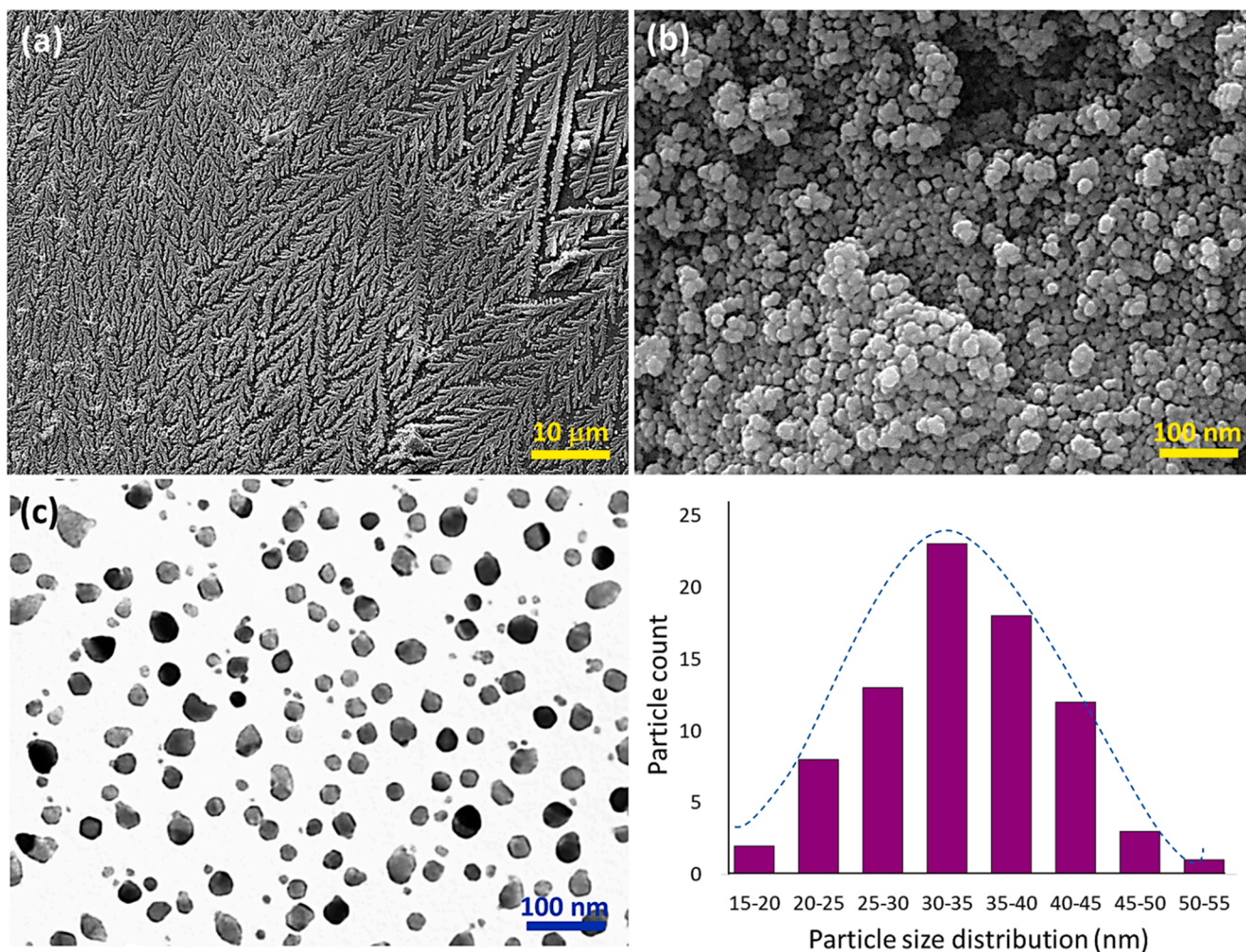


Fig. 6. (a,b) FESEM images, and (c) TEM image of the fabricated $\text{Cu}_2\text{O}/\text{Fe}_3\text{O}_4$ @guarana nanocomposite and size distribution diagram of metal oxide NPs.

intensity of the O—H groups (in the guarana's structure), which has been appeared at $\sim 3400\text{ cm}^{-1}$, was decreased through the composition with Fe_3O_4 and Cu_2O NPs. Also, the peaks related to Fe—O and Cu—O bands have been appeared at $\sim 600\text{ cm}^{-1}$ that prove the formation of the metal oxide NPs [31]. The existence of the essential elements in the samples was also proven by energy-dispersive X-ray (EDX) spectroscopy [32]. As demonstrated in Fig. 3(b), 13.0 and 8.8% of the total weight in the fabricated $\text{Cu}_2\text{O}/\text{Fe}_3\text{O}_4$ @guarana nanocomposite belong to iron and copper elements, respectively. In the EDX spectra, high similarity is observed, only copper's peak has been added in the spectrum (II), which is related to the fabricated $\text{Cu}_2\text{O}/\text{Fe}_3\text{O}_4$ @guarana nanocomposite.

Thermal resistance of the neat guarana (curve I), Fe_3O_4 @guarana (curve II), and the fabricated $\text{Cu}_2\text{O}/\text{Fe}_3\text{O}_4$ @guarana nanocomposite (curve III) has been studied by thermogravimetric analysis (TGA). As demonstrated in Fig. 4(a), the first shoulder is observed when guarana is dehydrated proportional to the increase in temperature until ca. $150\text{ }^\circ\text{C}$. Almost 7% of the weight has been lost at this stage. Then, the second shoulder, in which $\sim 50\%$ of the weight has been lost, is observed in a thermal range of $150\text{--}410\text{ }^\circ\text{C}$. At this stage, all the hydroxyl groups of guarana are removed as water molecules. As can be seen, the main decomposition is started after this stage. Considering the thermal resistance behaviors of the Fe_3O_4 @guarana and $\text{Cu}_2\text{O}/\text{Fe}_3\text{O}_4$ @guarana, this is clearly indicated that the thermal stability of guarana is enhanced through composition with the heterogeneous NPs. As can be seen in the TGA curves II and III, both main shoulders have shifted to higher temperatures. Magnetic property of the fabricated Fe_3O_4 @guarana and $\text{Cu}_2\text{O}/\text{Fe}_3\text{O}_4$ @guarana nanocomposite has also been studied by

vibrating-sample magnetometer (VSM) analysis (Fig. 4b). The S-shape curves prove super-paramagnetic behavior of the samples. As it can be seen in the M—H curves I and II, the magnetic feature of Fe_3O_4 @guarana is a bit reduced ($\sim 5\text{ emu/g}$) through the addition of the Cu_2O NPs. However, from the VSM curves (recorded at room temperature) this is well revealed that the fabricated catalytic system is quickly isolated from the mixture through applying a magnetic field.

The XRD pattern of the fabricated $\text{Cu}_2\text{O}/\text{Fe}_3\text{O}_4$ @guarana nanocomposite is shown in Fig. 5. As can be observed, the obtained diffraction pattern has been compared with the original patterns of the neat Fe_3O_4 , Cu_2O NPs, and guarana. It was clearly verified that the NPs have been well prepared and composited with guarana matrix. Accordingly, the peaks appeared at the angles $2\theta = 18.51^\circ$, 31.64° , 33.91° , 36.56° , 43.15° , 46.96° , 58.65° , 63.25° , 68.25° and 74.85° are attributed to the formed Fe_3O_4 and Cu_2O NPs [29,31]. Also, the broad peak initiated from $2\theta = 22^\circ$ and ended by ca. 48° and a peak appeared at ca. 72° are attributed to guarana matrix [33].

Morphology and particle size of the produced Fe_3O_4 and Cu_2O NPs were studied by field-emission scanning electron microscopy (FESEM) and transmission-electron microscopic (TEM) imaging methods (Fig. 6). As illustrated in image (a), the spherical-shaped Fe_3O_4 and Cu_2O NPs have been nicely distributed onto the guarana surfaces and formed a cluster-shaped nanocomposite. Moreover, the average size of the spherical NPs is obtained $\sim 40\text{ nm}$ diameter that confirms the obtained results from XRD analysis (image b). TEM was used for better discern of Fe_3O_4 and Cu_2O NPs (image c). As expected, some particles are relatively darker than the others in TEM image that are attributed to the

Cu₂O NPs due to more electron density of copper.

3. Experimental section

3.1. Materials and equipment

All the used materials and equipment in this work have been listed in Table S1 (in the SI section).

3.2. Methods

3.2.1. Preparation of Cu₂O/Fe₃O₄@guarana nanocomposite

In a three-necked round-bottom flask (100 mL), 3.0 g of guarana was placed and well dissolved in deionized water (25 mL) via ultrasonication, at 50 °C. After resulting a relative homogen mixture, FeCl₂·4H₂O (0.3 g, 1.5 mmol) and FeCl₃·6H₂O (0.5 g, 1.84 mmol) were added to the flask and the content were vigorously stirred for 60 min, at the same temperature. After 60 min stirring, an orange opaque solution is obtained. Afterward, the atmosphere of the flask was neutralized by N₂ gas and a solution of ammonia (10 mL, 1 M) was added drop by drop, during the stirring. The temperature was maintained at 50 °C during the addition of the ammonia. After completion of addition, the mixture were stirred for additional 2 h, at room temperature. Next, the reaction environment was neutralized by HCl (0.1 M) and CuCl₂·2H₂O (0.5 g, 2.92 mmol) was added into the flask. During the stirring at room temperature, ascorbic acid (1.13 mmol) was added. After 1 h stirring, the content was ultrasonicated in a cleaner bath (50 KHz, 150 W L⁻¹) for 10 min, and the resulting product (Cu₂O/Fe₃O₄@guarana) was magnetically separated (by holding a magnet at the bottom of the flask) and washed for several times with deionized water and finally dried.

3.2.2. General procedure for catalyzed synthesis of 2,4,5-triaryl-1H-imidazoles

An integration of substituted 4-chlorobenzaldehyde (0.14 g, 1 mmol), ammonium acetate (0.3 g, 4 mmol), benzyl (0.21 g, 1 mmol) and Cu₂O/Fe₃O₄@guarana nanocatalyst (0.01 g) was ultrasonicated in a cleaner bath (50 KHz, 150 W L⁻¹) in ethanol (3.0 mL) for 20 min. The reaction progress was monitored by thin layer chromatography (TLC) and after completion of the reaction, the catalyst was magnetically separated and washed with deionized water and dried. Flash-column chromatography was applied for purification of the desired products.

3.2.3. General procedure for catalyzed synthesis of 1,2,4,5-tetraryl-1H-imidazoles

An integration of benzyl (1 mmol), 4-chlorobenzaldehyde (1 mmol), benzyl amine (1 mmol) ammonium acetate (4 mmol), and Cu₂O/Fe₃O₄@guarana nanocatalyst (0.01 g) was ultrasonicated in a cleaner bath (50 KHz, 150 W L⁻¹) in ethanol (3.0 mL) for 20 min. The reaction progress was monitored by thin layer chromatography (TLC) (elution solvent: ethyl acetate/n-hexane 1:3). After completion of the reaction, the catalyst was magnetically separated and washed with deionized water and dried. Anti-solvent technique and in many cases flash-column chromatography was applied for purification of the desired products.

3.2.4. Spectral data for selected compounds

2-(4-Hydroxyphenyl)-4,5-diphenyl-1H-imidazole **6**. MP: 257–259 °C; ¹³C NMR (75 MHz, CDCl₃): δ_C (ppm); 170.5, 154.4, 135.0, 133.0, 132.0, 129.9, 129.8, 129.1, 128.8, 128.7, 128.6, 128.5, 128.2, 127.6, 126.5, 125.1; ¹H NMR (300 MHz, CDCl₃): δ_H (ppm); 9.72 (s, 1H), 8.00–7.25 (m, 14H), 4.44 (s, 1H).

2,4,5-Triphenyl-1H-imidazole **11**. Mp: 275–277 °C; ¹H NMR (300 MHz, DMSO-*d*₆): δ_H (ppm); 11.27 (s, 1H), 8.10 (d, 2H), 8.11 (d, 2H), 8.00–7.30 (m, 13H).

1-Benzyl-2-(4-chlorophenyl)-4,5-diphenyl-1H-imidazole **18**. MP: 160–163 °C; ¹³C NMR (75 MHz, CDCl₃): δ (ppm) = 146.8, 138.0, 135.3, 134.5, 131.7, 131.5, 131.3, 131.0, 130.5, 129.8, 129.5, 129.0, 128.1,

Table 1

Optimization of the reaction condition for the synthesis of 2-(4-chlorophenyl)-4,5-diphenyl-1H-imidazole.

Entry	Cat. system	Cat. weight (g)	Solvent	Temp. (°C)	Time (min)	Yield ^a (%)
1	Fe ₃ O ₄	0.01	EtOH	25	20	35
2	Guarana	0.01	EtOH	25	20	53
3	Fe ₃ O ₄ @guarana	0.01	EtOH	25	20	74
4	Cu ₂ O/ Fe ₃ O ₄ @guarana	0.005	EtOH	25	20	83
5	Cu ₂ O/ Fe ₃ O ₄ @guarana	0.01 ^b	EtOH	25	20	97*
6	Cu ₂ O/ Fe ₃ O ₄ @guarana	0.02	EtOH	25	20	97
7	Cu ₂ O/ Fe ₃ O ₄ @guarana	0.01	THF	25	20	92
8	Cu ₂ O/ Fe ₃ O ₄ @guarana	0.01	DMF	25	20	95
9	Cu ₂ O/ Fe ₃ O ₄ @guarana	0.01	Water	25	20	88
10	Cu ₂ O/ Fe ₃ O ₄ @guarana	0.01	EtOH	50	20	97
11	Cu ₂ O/ Fe ₃ O ₄ @guarana	0.01	EtOH	70	20	97

^a Isolated yield.

^b Based on the EDX data, 1.4 mol% of Cu is used in the catalyzed reactions (see the SI file, page S13).

* Optimum conditions. All reactions were carried out in an ultrasound cleaner bath (50 KHz, 150 W L⁻¹). 4-Chlorobenzaldehyde (1.0 mmol), benzyl (1.0 mmol), and ammonium acetate (2.0 mmol) were used in 3.0 mL of solvent.

127.2, 127.0, 126.5, 48.7; ¹H NMR (300 MHz, CDCl₃): δ (ppm) = 7.80 (d, 2H), 7.42–7.40 (m, 3H), 7.29–7.30 (m, 2H), 7.20–7.13 (m, 6H), 6.76 (d, 2H), 5.20 (s, 2H).

1-Benzyl-2-(3-methoxyphenyl)-4,5-diphenyl-1H-imidazole **21**. MP: 129–130 °C; ¹³C NMR (75 MHz, CDCl₃): δ (ppm) = 160, 147.8, 138.3, 137.8, 135.4, 132.9, 131.7, 131.4, 131.2, 130.5, 129.8, 129.7, 129.4, 128.9, 128.0, 127.1, 127.0, 126.5, 121.7, 115.6, 114.6, 55.9, 48.6, 41.1. ¹H NMR (300 MHz, CDCl₃): δ (ppm) = 7.48–7.46 (m, 2H), 7.41–7.40 (m, 3H), 7.32–7.30 (m, 3H), 7.21–7.20 (m, 5H), 7.19–7.15 (m, 3H), 7.15–6.81 (m, 1H), 6.80 (d, 2H), 5.16 (d, 2H), 3.70 (s, 3H).

3.3. Application of the Cu₂O/Fe₃O₄@guarana nanocomposite for catalyzing three- and four-component synthesis reactions of imidazole derivatives

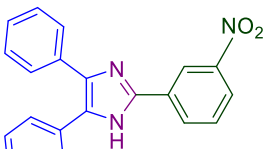
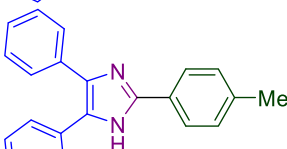
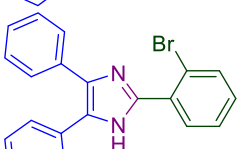
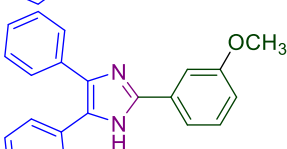
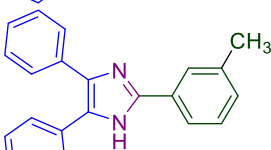
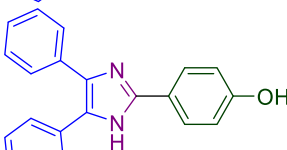
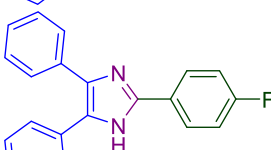
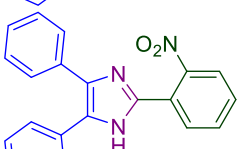
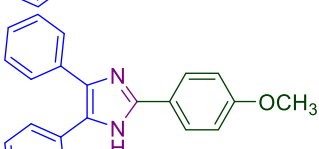
3.3.1. Optimization of the catalytic conditions for synthesis of the three component imidazole

In order to determine the best reaction conditions (solvent, temperature, and catalytic ratio of Cu₂O/Fe₃O₄@guarana), a model reaction was carried out using 4-chlorobenzaldehyde (1.0 mmol), benzyl (1.0 mmol), and ammonium acetate (2.0 mmol) in various solvents and different temperatures. Also, different amounts of the catalytic system were applied. A comparison was made between the performances of the Cu₂O/Fe₃O₄@guarana nanocomposite and the individual components as well. Table 1 summarize the obtained results from the optimization section.

3.3.2. Synthesis of the various derivatives of three component imidazole, under optimum catalytic conditions

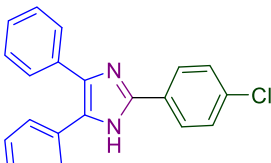
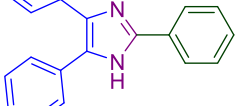
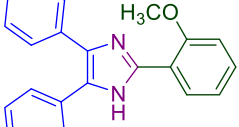
After optimization of the reaction conditions, various derivatives of three component imidazole were constructed by using various derivatives of benzaldehyde, in the presence of Cu₂O/Fe₃O₄@guarana nanocomposite. Thin-layer chromatography (TLC) was used to monitor the reaction progress. After completion of the reactions, the magnetic heterogeneous nanocatalyst were removed through holding an external magnet at the bottom of the reaction flask. The, flash-column chromatography was applied for further purification of the resulted products.

Table 2
 Synthesis of various derivatives of 2,4,5-triaryl-1H-imidazoles in the presence of Cu₂O/Fe₃O₄@guarana nanocomposite.

Entry	Product structure	Product No.	Yield ^a (%)	MP (°C)		Lit. ref.
				Found	Lit.	
1		1	89	264–266	265–266	[34]
2		2	86	230–231	230–231	[35]
3		3	85	199–201	200–201	[36]
4		4	87	259–260	258–260	[37]
5		5	81	298–299	296–299	[38]
6		6	83	257–259	257–258	[36]
7		7	87	197–199	196–198	[39]
8		8	75	229–231	230–231	[34]
9		9	88	229–231	230–231	[35]
10		10	97	258–260	259–262	[40]

(continued on next page)

Table 2 (continued)

Entry	Product structure	Product No.	Yield ^a (%)	MP (°C)		Lit. ref.
				Found	Lit.	
11		11	85	275–277	273–275	[37]
12		12	80	210–211	210–212	[41]
13		13	84	266	264–265	[34]

^a Isolated Yield.

Table 3

Optimization of the reaction condition for the synthesis of 1-benzyl-2-(4-chlorophenyl)-4,5-diphenyl-1H-imidazole.

Entry	Cat. system	Cat. weight (g)	Solvent	Temp. (°C)	Time (min)	Yield ^a (%)
1	Fe ₃ O ₄	0.02	EtOH	25	20	28
2	Guarana	0.02	EtOH	25	20	39
3	Fe ₃ O ₄ @guarana	0.02	EtOH	25	20	70
4	Cu ₂ O/ Fe ₃ O ₄ @guarana	0.01	EtOH	25	20	83
5	Cu ₂ O/ Fe ₃ O ₄ @guarana	0.02	EtOH	25	20	95*
6	Cu ₂ O/ Fe ₃ O ₄ @guarana	0.03	EtOH	25	20	95
7	Cu ₂ O/ Fe ₃ O ₄ @guarana	0.02	THF	25	20	90
8	Cu ₂ O/ Fe ₃ O ₄ @guarana	0.02	DMF	25	20	93
9	Cu ₂ O/ Fe ₃ O ₄ @guarana	0.02	Water	25	20	88
10	Cu ₂ O/ Fe ₃ O ₄ @guarana	0.02	EtOH	50	20	95
11	Cu ₂ O/ Fe ₃ O ₄ @guarana	0.02	EtOH	70	20	95

^a Isolated yield.

* Optimum conditions. All reactions were carried out in an ultrasound cleaner bath (50 KHz, 150 W L⁻¹). 4-Chlorobenzaldehyde (1.0 mmol), benzyl amine (1 mmol), benzyl (1.0 mmol), and ammonium acetate (2.0 mmol) were used in 3.0 mL of solvent.

Melting points of the obtained products were precisely compared with the literature. Some of them were also selected for more identification by ¹HNMR and ¹³CNMR spectroscopy. However, Table 2 marks the synthesized imidazole products under optimal catalytic conditions, with more details.

3.3.3. Optimization of the catalytic conditions for the synthesis of the four component imidazole

In order to extend the catalytic scope of the magnetic nanocatalyst, synthesis of the four component imidazole derivatives, with different parameters including temperature, solvent and amount of nanocatalyst was evaluated to determine the optimized reaction condition (Table 3, entries 1–11). For this purpose, a reaction mixture consists of benzyl (1 mmol), 4-chlorobenzaldehyde (1 mmol), benzyl amine (1 mmol) ammonium acetate (4 mmol) was considered as a model reaction. As shown in Table 3, entry 4–6 various amounts of catalyst loading are investigated and the 0.02 g was the highest yield percentage of the product. Also, increasing temperature was effectless to the yield of the reaction and the 25 °C was the best chosen (Table 3, entries 10 and 11). Furthermore, it was found that ethanol solvent is the best solvent in yield percentage of the product (Table 3, entries 7–9).

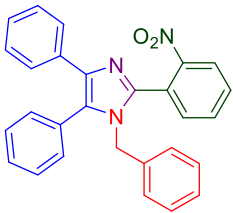
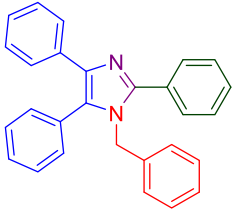
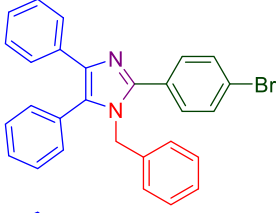
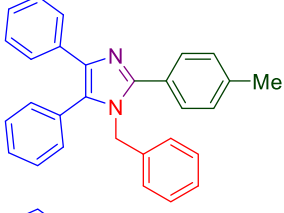
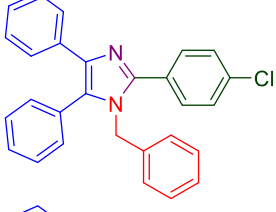
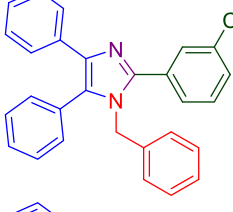
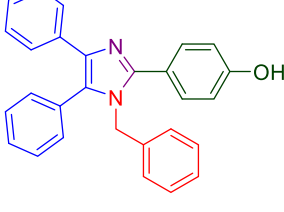
3.3.4. Synthesis of the various derivatives of 1,2,4,5-tetraryl-1H-imidazoles under optimum catalytic conditions

Having the optimized conditions, with purpose study performance of the Cu₂O/Fe₃O₄@guarana nanocomposite in the 1,2,4,5-tetraryl-1H-imidazoles reactions various derivatives as electron withdrawing and electron releasing was investigated. As be seen in Table 4, electron-withdrawing derivatives better than electron releasing derivatives converted to the desired product.

3.3.5. Comparison of the catalytic performance of Cu₂O/Fe₃O₄@guarana nanocomposite in the 2,4,5-triaryl-1H-imidazoles and 1,2,4,5-tetraryl-1H-imidazoles reactions with previously reported systems

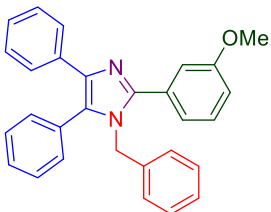
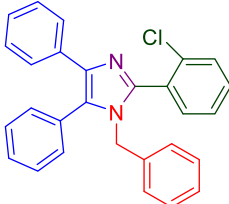
A brief survey on recently reported catalytic systems, which have been applied for the synthesis of the imidazole derivatives, was also done to highlight the efficiency of the fabricated Cu₂O/Fe₃O₄@guarana catalytic system. As seen in Table 5, higher reaction yield was obtained in shorter reaction time, for 2-(4-chlorophenyl)-4,5-diphenyl-1H-

Table 4
 Synthesis of various derivatives of 1,2,4,5-tetraphenyl-1H-imidazoles in the presence of Cu₂O/Fe₃O₄@guarana nanocomposite.

Entry	Product structure	Product No.	Yield ^a (%)	MP (°C)		Lit. ref.
				Found	Lit.	
1		14	71	151–152	152–155	[42]
2		15	81	163–165	165	[43]
3		16	89	173–175	175–178	[44]
4		17	87	163–164	163–165	[36]
5		18	95	160–163	162–165	[42]
6		19	88	144–148	146–148	[45]
7		20	82	134–137	135–137	[36]
8		21	86	129–130	129–131	[36]

(continued on next page)

Table 4 (continued)

Entry	Product structure	Product No.	Yield ^a (%)	MP (°C)		Lit. ref.
				Found	Lit.	
9		22	83	138–141	140–142	[45]
						

^a Isolated Yield.

Table 5

Comparison of the different catalytic systems applied for the synthesis of 2-(4-chlorophenyl)-4,5-diphenyl-1H-imidazole (10) and 1-benzyl-2-(4-chlorophenyl)-4,5-diphenyl-1H-imidazole (18).

Entry	Cat. System		Conditions	Time (min)	Yield (%)	Ref.
	Three component	Four component				
1	Yb(OPf) ₃	–	Perfluorodecalin/80 °C	360	83	[46]
2	Montmorillonite K10	–	EtOH/reflux	95	75	[47]
3	SBSSA ^a	–	Solvent free/130 °C	30	90	[48]
4	DBSA ^b	–	H ₂ O/reflux	240	75	[49]
5	–	4-(1-Imidazolium) butane sulfonate	Solvent free/80 °C	300	78	[50]
6	–	Acetic acid	EtOH/reflux	180	69	[51]
7	–	[bmim] ₃ [GdCl ₆]	Solvent free/120 °C	120	94	[52]
8	–	OAc-HPro@Fe ₃ O ₄	EtOH/60 °C	420	80	[53]
9	Cu ₂ O/Fe ₃ O ₄ @guarana	Cu ₂ O/Fe ₃ O ₄ @guarana	EtOH/ultrasonic/r.t.	20	97	–

^a Silica-bonded S-Sulfonic Acid.

^b Dodecylbenzenesulfonic acid.

imidazole **10** and 1-benzyl-2-(4-chlorophenyl)-4,5-diphenyl-1H-imidazole **18**, through using our catalytic system. In addition, it is clear that a milder reaction conditions was applied in this work.

3.3.6. Suggested mechanism

From mechanistic aspect, initially, the present Cu atoms in the structure of the catalyst activate the carbonyl group of aldehyde. Then, this activated form is converted to a diamine by ammonium acetate (stage 1 and 2). The benzyl groups is also activated by copper through the electronic interaction (stage 3) and reacts with the formed diamine, and a water molecule is removed (stage 4). During stage 5 the product is obtained and the catalytic system is separated and recycled [54,55]. A schematic of this plausible mechanism is illustrated in Fig. 7.

3.3.7. Catalyst reusability

The catalytic efficiency of the fabricated Cu₂O/Fe₃O₄@guarana nanocomposite was monitored in the model reaction after six times recycling. For this aim, after run 1, the Cu₂O/Fe₃O₄@guarana NPs were isolated from the reaction mixture and washed with ethanol for several times and reused for further running the process. In Fig. 8 it is observed that the nanocatalyst could be re-applied for additional five times without any considerable reduction in the catalytic performance. The FT-IR spectrum of the recovered nanocatalyst after six times usages has been shown in supporting information section (Fig. S9). From the TGA curve of the recovered catalyst (Fig. S10, in the SI file), it has been revealed that only 0.0092 mmol/g of guarana is lost after six times recycling, which confirms high stability of the prepared Cu₂O/

Fe₃O₄@guarana nanocomposite. The TGA estimations related to the fresh and recovered catalyst have been given in the SI file, on page S12.

4. Conclusions

Following the extensive research on the novel heterogeneous catalytic systems, we intended to prepare a nature-based hybrid nanocomposite with high magnetic property in nano scale and apply it in the organic synthesis reactions. In this regard, we chose “guarana” as a natural polymeric basis, which includes excellent biocompatibility. Fe₃O₄ and Cu₂O NPs have been further well immobilized into this natural matrix to add well magnetic behavior and promising catalytic efficiency to this catalytic system, respectively. Afterward, the application of this catalyst was precisely investigated in multicomponent (three- and four-component) synthesis reactions of imidazole derivatives. Concisely, it has been well shown that pure products with high reaction yields (97% and 95%) are obtained in a short reaction time (20 min) through applying this catalytic system under ultrasound wave irradiation with a specific frequency and power density. In summary, all of the distinguished properties of our novel designed product (Cu₂O/Fe₃O₄@guarana nanocomposite) such as high heterogeneity, excellent magnetic behavior, nano scale and cluster-shaped morphology, great thermal stability, well composition, and etc. have been studied by various analytical methods. Moreover, noticeable recyclability of this catalyst has been studied in this report. As well the characterization of the imidazole products have been done by ¹HNMR and ¹³CNMR spectroscopy.

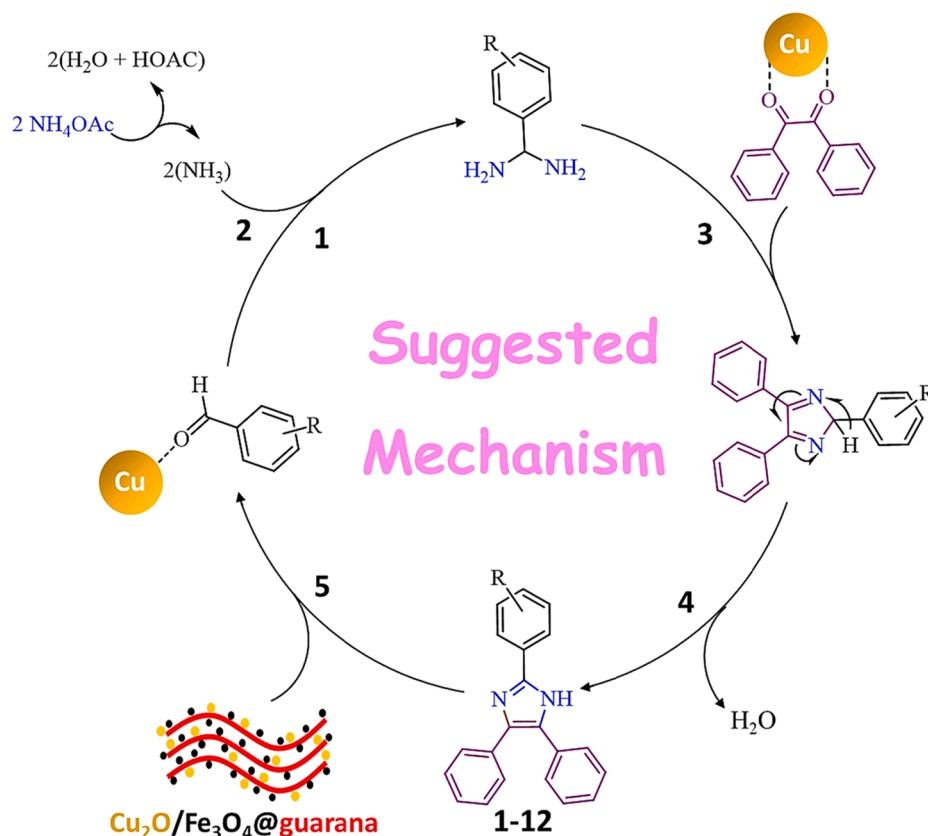


Fig. 7. The plausible mechanism for the synthesis of imidazole derivatives assisted by $\text{Cu}_2\text{O}/\text{Fe}_3\text{O}_4@guarana$ nanocomposite.

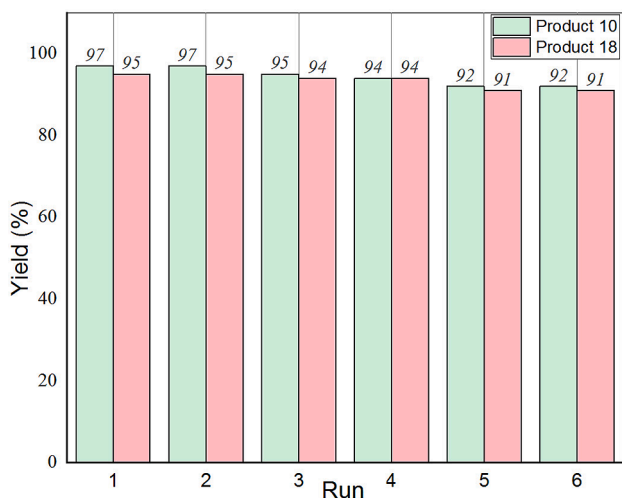


Fig. 8. Reusability diagram of $\text{Cu}_2\text{O}/\text{Fe}_3\text{O}_4@guarana$ nanocomposite.

CRedit authorship contribution statement

Zahra Varzi: Conceptualization, Investigation. **Mir Saeed Esmaeili:** Conceptualization, Methodology, Investigation. **Reza Taheri-Ledari:** Investigation, Writing - original draft, Writing - review & editing. **Ali Maleki:** Funding acquisition, Resources, Supervision.

Declaration of Competing Interest

The authors declare that they have no known competing financial interests or personal relationships that could have appeared to influence the work reported in this paper.

Acknowledgements

The authors gratefully acknowledge the partial support from the Research Council of the Iran University of Science and Technology.

Appendix A. Supplementary material

The SI file includes the NMR (H and C) of selected imidazole products and also FT-IR results of the recovered nanocatalyst. The brand and purity of used materials are also listed in this section. This section can be found in the online version Supplementary data to this article can be found online at <https://doi.org/10.1016/j.inoche.2021.108465>.

References

- [1] W. Zhang, R. Taheri-Ledari, Z. Hajizadeh, E. Zolfaghari, M.R. Ahghari, A. Maleki, M.R. Hamblin, Y. Tian, Enhanced activity of vancomycin by encapsulation in hybrid magnetic nanoparticles conjugated to a cell-penetrating peptide, *Nanoscale* 12 (2020) 3855–3870.
- [2] S. Parvaz, R. Taheri-Ledari, M.S. Esmaeili, M. Rabbani, A. Maleki, A brief survey on the advanced brain drug administration by nanoscale carriers: With a particular focus on AChE reactivators, *Life Sci.* 240 (2020) 117099.
- [3] R. Taheri-Ledari, W. Zhang, M. Radmanesh, S.S. Mirmohammadi, A. Maleki, N. Cathcart, V. Kitaev, Multi-stimuli nanocomposite therapeutic: docetaxel targeted delivery and synergies in treatment of human breast cancer tumor, *Small* 16 (2020) 2002733.
- [4] R. Taheri-Ledari, K. Valadi, A. Maleki, High-performance HTL-free perovskite solar cell: An efficient composition of ZnO NRs, RGO, and CuInS_2 QDs, as electron-transporting layer matrix, *Prog. Photovolt. Res. Appl.* 28 (2020) 956–970.
- [5] W. Futako, T. Sugawara, T. Kamiya, I. Shimizu, High electric field photocurrent of Vidicon and diode devices using wide band gap a-Si: H prepared with intentional control of silicon network by chemical annealing, *J. Organomet. Chem.* 611 (2000) 525–530.
- [6] M.S. Esmaeili, M.R. Khodabakhshi, A. Maleki, Z. Varzi, Green, natural and low cost Xanthum Gum supported Fe_3O_4 as a robust biopolymer nanocatalyst for the one-pot synthesis of 2-amino-3-cyano-4H-pyran derivatives, *Polycycl. Aromat.* (2020), <https://doi.org/10.1080/10406638.2019.1708418>.
- [7] A. Maleki, F. Hassanzadeh-Afruzi, Z. Varzi, M.S. Esmaeili, Magnetic dextrin nanobiomaterial: an organic-inorganic hybrid catalyst for the synthesis of

- biologically active polyhydroquinoline derivatives by asymmetric Hantzsch reaction, *Mater. Sci. Eng. C* 109 (2020) 110502.
- [8] A. Maleki, R. Taheri-Ledari, M. Soroushnejad, Surface functionalization of magnetic nanoparticles via palladium-catalyzed Diels-Alder approach, *ChemistrySelect* 3 (2018) 13057–13062.
- [9] M. Gholinejad, N. Jeddi, Copper nanoparticles supported on agarose as a bioorganic and degradable polymer for multicomponent click synthesis of 1,2,3-triazoles under low copper loading in water, *ACS Sustainable Chem. Eng.* 2 (2014) 2658–2665.
- [10] A. Maleki, Z. Varzi, F. Hassanzadeh-Afruzi, Preparation and characterization of an eco-friendly $ZnFe_2O_4$ @ alginate nanocomposite catalyst and its application in the synthesis of 2-amino-3-cyano-4H-pyran derivatives, *Polyhedron* 171 (2019) 193–203.
- [11] M. Gholinejad, F. Saadati, S. Shaybanizadeh, B. Pullithadathil, Copper nanoparticles supported on starch micro particles as a degradable heterogeneous catalyst for three-component coupling synthesis of propargylamines, *RSC Adv.* 6 (2016) 4983–4991.
- [12] A. Ghaderi, M. Gholinejad, H. Firouzabadi, Palladium deposited on naturally occurring supports as a powerful catalyst for carbon-carbon bond formation reactions, *Curr. Org. Chem.* 20 (2016) 327–348.
- [13] R. Taheri-Ledari, A. Maleki, E. Zolfaghari, M. Radmanesh, H. Rabbani, A. Salimi, R. Fazel, High-performance sono/nano-catalytic system: Fe_3O_4 @Pd/CaCO₃-DTT core/shell nanostructures, a suitable alternative for traditional reducing agents for antibodies, *Ultrason. Sonochem.* 61 (2020) 104824.
- [14] R. Taheri-Ledari, S.M. Hashemi, A. Maleki, High-performance sono/nano-catalytic system: CTSN/ Fe_3O_4 -Cu nanocomposite, a promising heterogeneous catalyst for the synthesis of N-arylimidazoles, *RSC Adv.* 9 (2019) 40348–40356.
- [15] A. Maleki, R. Taheri-Ledari, R. Ghalavand, R. Firouzi-Haji, Palladium-decorated o-phenylenediamine-functionalized Fe_3O_4 /SiO₂ magnetic nanoparticles: A promising solid-state catalytic system used for Suzuki-Miyaura coupling reactions, *J. Phys. Chem. Solids* 136 (2020) 109200.
- [16] M. Bagherzadeh, M. Bahjati, A. Mortazavi-Manesh, Synthesis, characterization and catalytic activity of supported vanadium Schiff base complex as a magnetically recoverable nanocatalyst in epoxidation of alkenes and oxidation of sulphides, *J. Organomet. Chem.* 897 (2019) 200–206.
- [17] R. Taheri-Ledari, A. Maleki, Antimicrobial therapeutic enhancement of levofloxacin via conjugation to a cold-penetrating peptide: An efficient sonochemical catalytic process, *J. Pept. Sci.* 26 (2020) e3277.
- [18] S. Luo, D. Nie, Z. Li, X. Sun, L. Hu, X. Liu, Effects of carboxylic acid auxiliary ligands on the magnetic properties of azido-Cu(II) complexes: A density functional theory study, *Polyhedron* 182 (2020) 114506.
- [19] M.S. Esmaili, Z. Varzi, R. Taheri-Ledari, A. Maleki, Preparation and study of the catalytic application in the synthesis of xanthenedione pharmaceuticals of a hybrid nano-system based on copper, zinc and iron nanoparticles, *Res. Chem. Intermed.* (2020), <https://doi.org/10.1007/s11164-020-04311-8>.
- [20] A. Maleki, R. Taheri-Ledari, R. Ghalavand, Design and fabrication of a magnetite-based polymer-supported hybrid nanocomposite: A promising heterogeneous catalytic system utilized in known Palladium-assisted coupling reactions, *Comb. Chem. High. T Scr.* 23 (2020) 119–125.
- [21] R. Taheri-Ledari, M.S. Esmaili, Z. Varzi, R. Eivazzadeh-Keihan, A. Maleki, A. E. Shalan, Facile route to synthesize Fe_3O_4 @acacia-SO₃H nanocomposite as a heterogeneous magnetic system for catalytic applications, *RSC Adv.* 10 (2020) 40055–40067.
- [22] Z. Varzi, A. Maleki, Design and preparation of ZnS - $ZnFe_2O_4$: a green and efficient hybrid nanocatalyst for the multicomponent synthesis of 2,4,5-triaryl-1-H-imidazoles, *Appl. Organomet. Chem.* 33 (2019) e5008.
- [23] K. Valadi, S. Gharibi, R. Taheri-Ledari, A. Maleki, Ultrasound-assisted synthesis of 1, 4-dihydropyridine derivatives by an efficient volcanic-based hybrid nanocomposite, *Solid State Sci.* 101 (2020) 106141.
- [24] R. Taheri-Ledari, J. Rahimi, A. Maleki, Synergistic catalytic effect between ultrasound waves and pyrimidine-2,4-diamine-functionalized magnetic nanoparticles: Applied for synthesis of 1,4-dihydropyridine pharmaceutical derivatives, *Ultrason. Sonochem.* 59 (2019) 104737.
- [25] R. Mozafari, F. Heidarzadeh, F. Nikipour, $MnFe_2O_4$ magnetic nanoparticles modified with chitosan polymeric and phosphotungstic acid as a novel and highly effective green nanocatalyst for regio- and stereoselective synthesis of functionalized oxazolidin-2-ones, *Mater. Sci. Eng. C* 105 (2019) 110109.
- [26] J. Safari, M. Tavakoli, M.A. Ghasemzadeh, A highly effective synthesis of pyrimido [4,5-b]quinoline-tetraones using $H_3PW_{12}O_{40}$ /chitosan/ $NiCo_2O_4$ as a novel magnetic nanocomposite, *Polyhedron* 182 (2020) 114459.
- [27] S. Salek Soltani, R. Taheri-Ledari, S.M.F. Farnia, A. Maleki, A. Foroumadi, Synthesis and characterization of a supported Pd complex on volcanic pumice laminates textured by cellulose for facilitating Suzuki-Miyaura cross-coupling reactions, *RSC Adv.* 10 (2020) 23359–23371.
- [28] D. Mudgil, S. Barak, B.S. Khatkar, Guar gum: processing, properties and food applications-A Review, *J. Food Sci. Tech.* 51 (2014) 409–418.
- [29] J. Rahimi, R. Taheri-Ledari, M. Niksefat, A. Maleki, Enhanced reduction of nitrobenzene derivatives: Effective strategy executed by Fe_3O_4 /PVA-10%Ag as a versatile hybrid nanocatalyst, *Catal. Comm.* 134 (2020) 105850.
- [30] A. Maleki, R. Taheri-Ledari, J. Rahimi, M. Soroushnejad, Z. Hajizadeh, Facile peptide bond formation: Effective interplay between isothiazolone rings and silanol groups at silver/iron oxide nanocomposite surfaces, *ACS Omega* 4 (2019) 10629–10639.
- [31] M.S. Esmaili, Z. Varzi, R. Eivazzadeh-Keihan, A. Maleki, H. Ghafari, Design and development of natural and biocompatible raffinose-Cu₂O magnetic nanoparticles as a heterogeneous nanocatalyst for the selective oxidation of alcohols, *Mol. Catal.* 492 (2020) 111037.
- [32] R. Taheri-Ledari, J. Rahimi, A. Maleki, Method screening for conjugation of the small molecules onto the vinyl-coated Fe_3O_4 /silica nanoparticles: highlighting the efficiency of ultrasonication, *Mater. Res. Express* 7 (2020) 015067.
- [33] D. Mudgil, S. Barak, B.S. Khatkar, X-ray diffraction, IR spectroscopy and thermal characterization of partially hydrolyzed guar gum, *Int. J. Biol. Macromol.* 50 (2012) 1035–1039.
- [34] A. Maleki, Z. Alirezvani, A Highly efficient synthesis of substituted imidazoles via a one-pot multicomponent reaction by using urea/hydrogen peroxide (UHP), *J. Chil. Chem. Soc.* 61 (2016) 3.
- [35] A. Shaabani, A. Maleki, M. Behnam, Tandem oxidation process using ceric ammonium nitrate: Three-component synthesis of trisubstituted imidazoles under aerobic oxidation conditions, *Syn. Comm.* 39 (2009) 102–110.
- [36] M. Esmailpour, J. Javidi, F. Dehghani, S. Zahmatkesh, One-pot synthesis of multisubstituted imidazoles catalyzed by Dendrimer-PWAn nanoparticles under solvent-free conditions and ultrasonic irradiation, *Res. Chem. Intermed.* 43 (2017) 163–185.
- [37] R. Mirsafaei, M.M. Heravi, S. Ahmadi, T. Hosseinejad, Synthesis and properties of novel reusable nano-ordered KIT-5-N-sulfamic acid as a heterogeneous catalyst for solvent-free synthesis of 2,4,5-triaryl-1-H-imidazoles, *Chem. Pap.* 70 (2016) 418–429.
- [38] H. Naeimi, D. Aghaseydekarimi, Ionophore silica-coated magnetite nanoparticles as a recyclable heterogeneous catalyst for one-pot green synthesis of 2,4,5-trisubstituted imidazoles, *Dalton Trans.* 45 (2016) 1243–1253.
- [39] A. Maleki, H. Movaheda, R. Paydar, Design and development of a novel cellulose/ γ - Fe_2O_3 /Ag nanocomposite: a potential green catalyst and antibacterial agent, *RSC Adv.* 6 (2016) 13657–13665.
- [40] J.N. Sangshetti, N.D. Kokare, S.A. Kotharkar, D.B. Shinde, Sodium bisulfite as an efficient and inexpensive catalyst for the one-pot synthesis of 2,4,5-Triaryl-1H-imidazoles from benzil or benzoin and aromatic aldehydes, *Monatsh. Chem.* 139 (2008) 125–127.
- [41] M. Yar, M. Bajda, S. Shahzad, N. Ullah, M.A. Gilani, M. Ashraf, A. Rauf, A. Shaukat, Organocatalyzed solvent free an efficient novel synthesis of 2,4,5-trisubstituted imidazoles for a-glucosidase inhibition to treat diabetes, *Bioorg. Chem.* 58 (2015) 65–71.
- [42] B. Sadeghi, B.B.F. Mirjalili, M.M. Hashemi, $BF_3 \cdot SiO_2$: an efficient reagent system for the one-pot synthesis of 1,2,4,5-tetrasubstituted imidazoles, *Tetrahedron Lett.* 49 (2008) 2575–2577.
- [43] M.M. Heravi, F. Derikvan, F.F. Bamoharram, Highly efficient, four-component one-pot synthesis of tetrasubstituted imidazoles using Keggin-type heteropolyacids as green and reusable catalysts, *J. Mol. Catal. A. Chem.* 263 (2007) 112–114.
- [44] M. Salimi, M.A. Nasser, T.D. Chapesshloo, B. Zakerinasab, (Carboxy-3-oxopropylamino)-3-propylsilylcellulose as a novel organocatalyst for the synthesis of substituted imidazoles under solvent-free conditions, *RSC Adv.* 5 (2015) 33974–33980.
- [45] S. Kantevari, S.V.N. Vuppalapati, D.O. Biradar, L. Nagarapu, Highly efficient, one-pot, solvent-free synthesis of tetrasubstituted imidazoles using $HClO_4$ - SiO_2 as novel heterogeneous catalyst, *J. Mol. Catal. A. Chem.* 266 (2007) 109–113.
- [46] M.G. Shen, C. Cai, W.B. Yi, Ytterbium perfluorooctanesulfonate as an efficient and recoverable catalyst for the synthesis of trisubstituted imidazoles, *J. Fluor. Chem.* 129 (2008) 541–544.
- [47] A. Teimouria, A.N. Chermahini, An efficient and one-pot synthesis of 2,4,5-trisubstituted and 1,2,4,5-tetrasubstituted imidazoles catalyzed via solid acid nanocatalyst, *J. Mol. Catal. A-Chem.* 346 (2011) 39–45.
- [48] K. Niknam, M.R. Mohammadzadeh, S. Mirzaee, D. Saberi, Silica-bonded S-sulfonic acid: a recyclable catalyst for the synthesis of trisubstituted imidazoles under solvent-free conditions, *Chinese J. Chem.* 28 (2010) 663–669.
- [49] B. Das, J. Kashanna, R.A. Kumar, P. Jangili, Synthesis of 2,4,5-trisubstituted and 1,2,4,5-tetrasubstituted imidazoles in water using p-dodecylbenzenesulfonic acid as catalyst, *Monatsh. Chem.* 144 (2013) 223–226.
- [50] M.R.A.K. Bagdi, D. Kundu, A. Majee, A. Hajra, Zwitterionic-Type Molten Salt Catalyzed Multicomponent Reactions: One-Pot Synthesis of Substituted Imidazoles Under Solvent-Free Conditions, *J. Heterocycl. Chem.* 49 (2012) 1224–1228.
- [51] Z.G. Song, X. Wan, S. Zhao, A modified procedure for the synthesis of 2,4,5-tri- and 1,2,4,5-tetrasubstituted imidazoles, *Chem. Nat. Compd.* 48 (2013) 1119–1121.
- [52] A. Akbari, Tri(1-butyl-3-methylimidazolium) gadolinium hexachloride, ([bmim]₃)[GdCl₆], a magnetic ionic liquid as a green salt and reusable catalyst for the synthesis of tetrasubstituted imidazoles, *Tetrahedron Lett.* 57 (2016) 431–434.
- [53] H. Aghahosseini, A. Ramazani, K. Slepokura, T. Lis, The first protection-free synthesis of magnetic bifunctional L-proline as a highly active and versatile artificial enzyme: synthesis of imidazole derivatives, *J. Colloid Interface Sci.* 511 (2018) 222–232.
- [54] S. Pervaiz, S. Mutahir, I.U. Khan, M. Ashraf, X. Liu, S. Tariq, B. Zhou, M.A. Khan, Organocatalyzed solvent free and efficient synthesis of 2,4,5-trisubstituted imidazoles as potential acetylcholinesterase inhibitors for Alzheimer's disease, *Chem. Biodivers.* 17 (2020) e1900493.
- [55] J.J. Gabla, S.R. Mistry, K.C. Maheria, An efficient green protocol for the synthesis of tetra-substituted imidazoles catalyzed by zeolite BEA: effect of surface acidity and polarity of zeolite, *Catal. Sci. Technol.* 7 (2017) 5154–5167.